

# MODULATED MEASUREMENT MATRIX DESIGN FOR COMPRESSED SENSING

Chunli Guo, Mike E. Davies

School of Engineering and Electronics, The University of Edinburgh  
 {c.guo, mike.davies}@ed.ac.uk

## ABSTRACT

In this paper, we extend the idea of the seeding matrix design and introduce the modulated matrix framework for compressed sensing. The 1-D state evolution equation is derived to track the sample distortion performance as a function of the signal distribution and the rescaling matrix. A special example, the two-block matrix, is presented as a generalization of the hybrid zeroing matrix. The first order phase transition is further studied to better understand the dynamics. With the two-block matrix, exact recovery can be achieved in the region where the homogeneous Gaussian matrix is not optimal for the sparse signals. For compressible signals, the reconstruction quality can also be effectively improved.

**Index Terms**— Sample distortion function, phase transition, modulated matrix, block state evolution equation

## 1. INTRODUCTION

The compressed sensing (CS) problem can be generalized as solving an underestimated linear system: Given the information of the measurement matrix  $\Phi \in \mathbb{R}^{M \times N}$ ,  $M < N$  and the observation vector  $Y = \Phi X$ , the objective is to obtain good estimation of the source signal  $X$ . The reconstruction quality for different choices of  $\Phi$  and reconstruction algorithm is quantified using the mean squared error (MSE) at certain sampling ratio  $\alpha = M/N$ , and is bounded by the sample distortion (SD) function as defined in [1].

Despite the general advantages of the homogeneous Gaussian matrix, there have recently been a number of studies on tailoring  $\Phi$  with the signal distribution and the reconstruction algorithm, aiming for better CS performance. Previously, a hybrid zeroing matrix was introduced by exploring the convex property of the SD function [2], [3]. It successfully convexifies the SD function in the low sampling regime, thus improving the reconstruction quality for the compressible signals. Krzakala and colleagues pioneered the use of the seeding measurement matrix [4]. Designed as the spatially-coupled block diagonal Gaussian matrix, it can obtain an exact reconstruction of the sparse signal under a sampling ratio approaching the theoretical limit.

In this paper, we extend the seeding matrix idea to a simple and effective design: the modulated matrix. Different from the block diagonal structure of the seeding matrix, the modulated matrix consists of several  $M$  row Gaussian matrices with different variance. By varying the variance for the sub-matrices, we are essentially reweighing the signal distribution. In the limit of large system sizes, we present a 1-D state evolution dynamical system to predict its performance with the AMP reconstruction algorithm, based on the work in [5], to complete the modulated matrix framework.

Chunli Guo gratefully acknowledge the Maxwell Advanced Technology Fund at the University of Edinburgh in funding her PhD studies.

Inspired by the hybrid zeroing matrix, we considered a special form of the modulated matrix, the two-block matrix. To better understand the effect of the two-block matrix, we analysed the first order phase transition (FOPT), as observed in [6], from the state evolution perspective. The necessary and sufficient condition for signals without FOPT is then derived. For sparse signals, which have a FOPT, the two-block matrix can break the phase transition limit of the homogeneous Gaussian matrix and achieve substantially better SD performance. For homogeneous Gaussian systems without FOPT, we show that the two-block matrix will retain this non-FOPT property. Setting the rescaling parameter as 0 and 1 for the two-block structure is empirically optimal.

The rest of the paper is organized as following. The modulated matrix framework is introduced in Section 2. The two-block matrix is explained in Section 3. Numerical simulation is provided in Section 4. We finish the paper with conclusion in Section 5.

## 2. MODULATED MATRIX FRAMEWORK

### 2.1. Review of the seeding matrices

Krzakala et al. suggested the seeding matrix design in [4], [5] and [6]. It was demonstrated both heuristically and numerically that the seeding matrix is able to reach the fundamental reconstruction limit for the sparse signal. The measurement matrix  $\Phi$  is divided into  $L_r \times L_c$  blocks with the size of each being  $M_q \times N_p$ ,  $q = 1, \dots, L_r$ ,  $p = 1, \dots, L_c$ . For each block, the components are drawn i.i.d from the Gaussian distribution with zero mean and variance  $J_{qp}/N$ .

The MSE behaviour of the seeding matrix with the AMP-based reconstruction algorithm, i.e. the Bayesian optimal AMP [7] and the Generalized AMP (GAMP) [8], can be tracked by the state evolution (SE) equation. Based on the replica analysis, the SE equations for the seeding matrix form a  $2L_c$ -D dynamical system [5]:

$$E_p^{(t+1)} = \mathbb{E} \left\{ \left[ F \left( x + \frac{z}{\sqrt{\tau_p}}; \frac{1}{\tau_p} \right) - x \right]^2 \right\} \quad (1)$$

$$\tau_p = \sum_{q=1}^{L_r} \frac{M_q J_{qp}}{\sum_{r=1}^{L_c} J_{qr} N_r E_r^t} \quad (2)$$

where  $E_p^{(t+1)}$  is the reconstruction MSE for the  $p$ th signal block at the  $t + 1$  iteration.  $z \sim \mathcal{N}(0, 1)$  is independent of  $x$ . The function  $F(\cdot)$  is the non-linear scalar MMSE estimator of  $x$  given  $x + z$ . The expectation in (1) is taken with respect to both  $x$  and  $z$ . The SE equations provide accurate prediction for the reconstruction performance. They can also be used to optimize the matrix parameters.

## 2.2. Modulated matrices

In this section, we introduced the modulated matrix design, a variation of the seeding matrix, and derive its SE dynamics. Instead of dividing both columns and rows of the measurement matrix into blocks, the modulated matrix  $\Phi_M$  is composed of  $L_c$  M-row sub-matrices  $\Phi_i \in \mathbb{R}^{M \times N_i}$ ,  $i = 1, \dots, L_c$ ,  $\gamma_i = N_i/N$  and  $\sum_i N_i = N$ . Each consists of i.i.d random elements drawn from the Gaussian distribution with zero mean and  $J_i/N$  variance. Let us define the rescaling matrix  $\mathbf{R} \in \mathbb{R}^{N \times N}$  as:

$$\mathbf{R} = \begin{pmatrix} \sqrt{J_1} \mathbf{I}_1 & 0 & \cdots & 0 \\ 0 & \sqrt{J_2} \mathbf{I}_2 & \cdots & 0 \\ \vdots & \vdots & \ddots & \vdots \\ 0 & 0 & \cdots & \sqrt{J_{L_c}} \mathbf{I}_{N_{L_c}} \end{pmatrix} \quad (3)$$

where  $\mathbf{I}_i \in \mathbb{R}^{N_i \times N_i}$  is the identity matrix. The modulated matrix is then the product of the homogeneous Gaussian matrix  $\mathbf{G}$  and the rescaling matrix:

$$\Phi_M = \mathbf{G}\mathbf{R} \quad (4)$$

The state evolution for  $\Phi_M$  can be derived as a special case of the seeding matrix using (1), (2). To be specific,  $L_r = 1$ . For each block, we have:

$$E_i^t = S(\tau_i^t) \quad (5)$$

$$= \mathbb{E} \left\{ \left[ F(x + z\sqrt{\tau_i^t}; \tau_i^t) - x \right]^2 \right\} \quad (6)$$

$$\tau_i^{(t+1)} = \frac{\sum_k J_k \gamma_k S(\tau_k^t)}{\alpha J_i} \quad (7)$$

The total MSE for each iteration is the average over all blocks:

$$\bar{E}^t = \frac{1}{L_c} \sum_{r=1}^{L_c} E_r^t \quad (8)$$

Now we introduce a rescaled variable  $\hat{\tau} = J_i \tau_i$ , which is independent of the block index  $i$ . The update rule for  $\hat{\tau}$  becomes:

$$\hat{\tau}^{(t+1)} = \frac{\sum_k J_k \gamma_k S(\hat{\tau}^t / J_k)}{\alpha} \quad (9)$$

which is the SE equation for the modulated matrices. When the iteration of (9) converges to  $\hat{\tau}^*$ , the MSE at sampling ratio  $\alpha$  can be accurately predicted as

$$\bar{E} = \frac{1}{L_c} \sum_k S\left(\frac{\hat{\tau}^*}{J_k}\right) \quad (10)$$

We can also extend the aforementioned matrix design to the stochastic setting by introducing a random rescaling parameter  $J$  for each column. That is,  $L_c = N$  and  $J$  with the distribution  $p(J)$ . In the limit of large systems, the SE equation and the distortion prediction become

$$\hat{\tau}^{(t+1)} = \frac{1}{\alpha} \mathbb{E}_J \left\{ JS\left(\frac{\hat{\tau}^t}{J}\right) \right\} \quad (11)$$

$$\bar{E} = \mathbb{E}_J \left\{ S\left(\frac{\tau^*}{J}\right) \right\} \quad (12)$$

where the expectation is calculated with respect to  $J$ .

Both the deterministic (9) and stochastic (11) dynamics are described by a 1-D SE equation, which is a remarkable feature of the modulated matrix framework. It makes the analysis and the optimization of the modulated matrix much easier than the general seeded matrices of [4].

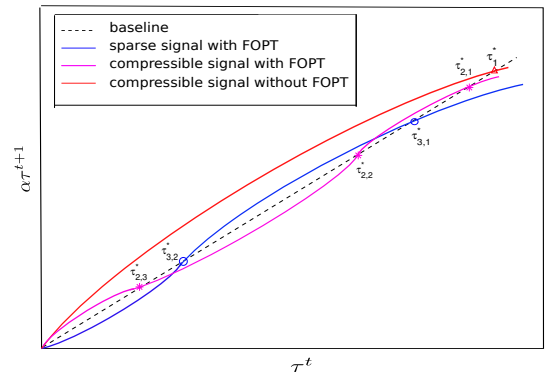


**Fig. 1.** The schematic plot of three types of SE behaviour to illustrate the FOPT. The dashline is the baseline  $\alpha\tau^t$ . The solid lines are the SE evolution  $\alpha\tau^{(t+1)} = S(\tau^t)$  for signals with the homogeneous Gaussian matrix. The number of non-zero intersection points with the baseline varies for different types of signals.

## 3. TWO-BLOCK MATRIX DESIGN

We have previously studied the convexity of the SD function and introduced the hybrid zeroing matrix [2], [3]. It has been illustrated analytically that in the concave SD region, better performance can be achieved by setting a portion of the measurement matrix to zero. Motivated by this design, we consider a simple form of the rescaling matrix

$$\hat{\mathbf{R}} = \begin{pmatrix} \mathbf{I}_1 & 0 \\ 0 & \sqrt{J_2} \mathbf{I}_2 \end{pmatrix} \quad (13)$$

We denote the corresponding  $\hat{\Phi}_M$  as the two-block matrix. Note that setting  $J_2 = 0$  and  $\gamma_1 = \alpha/\alpha_c$  for  $\alpha < \alpha_c$  with  $\alpha_c$  being the critical sampling ratio results in the hybrid zeroing matrix and the convexified SD function. Here, we consider  $J_2$  being non-zero and without loss of generality assume  $0 < J_2 < 1$ . The SE equation and the distortion equation for  $\hat{\Phi}_M$  become:

$$\hat{\tau}^{(t+1)} = \frac{1}{\alpha} M(\hat{\tau}^{(t+1)}) \quad (14)$$

$$= \frac{1}{\alpha} \left[ \gamma_1 S(\hat{\tau}^t) + (1 - \gamma_1) J_2 S\left(\frac{\hat{\tau}^t}{J_2}\right) \right] \quad (15)$$

$$\bar{E} = \gamma_1 S(\hat{\tau}^*) + (1 - \gamma_1) S\left(\frac{\hat{\tau}^*}{J_2}\right) \quad (16)$$

As observed in [6], the performance of the seeding matrix is highly related to the FOPT property of the source signal. In the following, we present the condition for signals without FOPT.

### 3.1. Phase transition analysis

The FOPT is a discontinuous drop of the MSE at a particular sampling ratio in the context of the SD framework. It can be observed for sparse signals and some signals with a good level of compressibility. In [6] the authors draw a connection between the SE dynamics and the potential function, and explained the FOPT by analysing the behaviour of the local maximas of the potential function. Here, we studied the phenomenon from the state evolution perspective.

To better illustrate the dynamics, a schematic plot for three typical types of SE behaviour with the homogeneous Gaussian matrix is presented in Fig. 1. The actual fixed points development for the

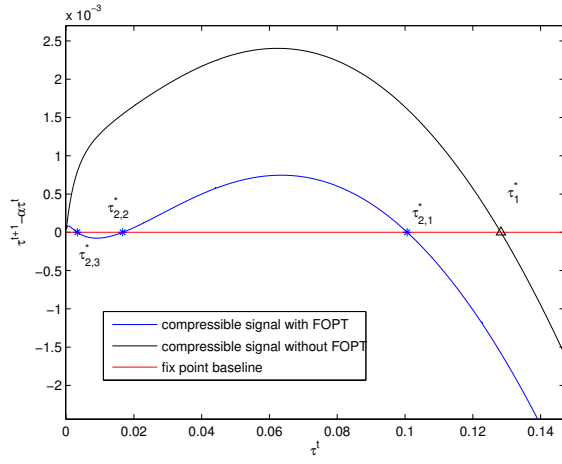


**Fig. 2.** Fixed points for the SE evolution  $\tau^{t+1} = S(\tau^t)/\alpha$  with homogeneous Gaussian matrix at sampling ratio  $\alpha = 0.58$ . For the compressible signal without FOPT,  $p(x) = 0.4\mathcal{N}(x; 0, 5 \times 10^{-3})$ , there is only one non-zero fixed point  $\tau_1^* = 0.1283$ . For the compressible signal with FOPT,  $p(x) = 0.4\mathcal{N}(x; 0, 5 \times 10^{-4})$ , three non-zero fixed points exist,  $\tau_{2,1}^* = 0.1006$ ,  $\tau_{2,2}^* = 0.0167$  and  $\tau_{2,3}^* = 3.3154 \times 10^{-3}$ .

compressible signal and the sparse signal are shown in Fig. 2 and Fig. 3, respectively.

For the compressible signal without FOPT, as we gradually increase  $\alpha$ , the intersection point of  $\alpha\tau^t$  and  $S(\tau^t)$  decreases continuously to zero as  $\alpha$  approaches 1. It leads to a smooth transition of  $\tau^*$  with respect to  $\alpha$ , thus a continuous SD curve. For the compressible signal with FOPT,  $S(\tau^t)$  consists of three smooth arcs, as demonstrated in Fig. 1. For a small  $\alpha$ , the SE iteration will always converge at the largest fix point  $\tau_{2,1}^*$  associated with the first concave arc. As  $\alpha$  increases, the baseline will surpass the first two arcs and intersect with the third one at  $\tau_{2,3}^*$ . Because of the existence of the convex curve between the two concave arcs, we cannot obtain a smooth transition between  $\tau_{2,1}^*$  and  $\tau_{2,3}^*$ , thus the FOPT occurs.

When using the homogeneous Gaussian encoder and the AMP decoder, sparse signals may also belong to the category of signals with FOPT, but their SE function behaves slightly differently. As illustrated in Fig. 1, its  $S(\tau^t)$  consists of a convex and a concave arc and intersects with the concave curve at fixed points  $\tau_{3,1}^*$  and  $\tau_{3,2}^*$  for some  $\alpha$ . Once  $\alpha$  is large enough for the two points to merge, the convergence point  $\tau^*$  will suddenly drop to zero as  $\alpha$  keeps increasing. A discontinuity of the MSE to zero is expected in the SD framework.

Thus the necessary and sufficient condition for signals without FOPT is for any  $\tau^*$ , the baseline  $\alpha\tau^*$  must always lie below the SE equation between 0 and  $\tau^*$ . Mathematically speaking, the slope of the baseline must be less than the gradient of the SE function for any  $\tau > 0$

$$\frac{f(\tau^*)}{\tau^*} < \eta(\tau^*), \quad \text{and} \quad \eta(\tau) = \frac{df(\tau)}{d\tau} \quad (17)$$

where  $\alpha\tau^{t+1} = f(\tau^t)$  is the general form of the SE equation.

### 3.2. The two-block matrix effect on phase transition

If the signal has FOPT with the homogeneous Gaussian matrix, the two-block matrix is able to accelerate the phase transition. With the

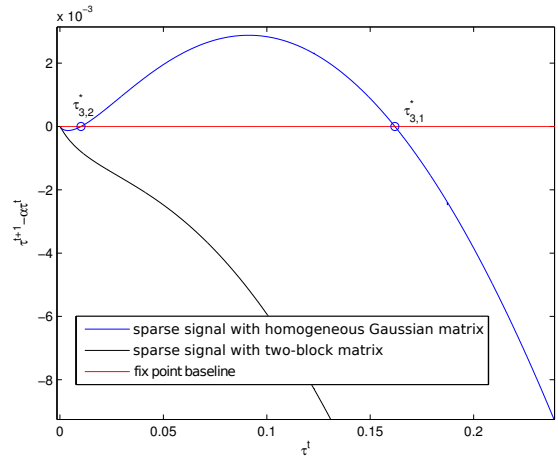


**Fig. 3.** The fixed points for the SE evolution with both homogeneous Gaussian matrix and the two-block matrix. The sparse signal is  $p(x) = 0.4\mathcal{N}(x; 0, 1) + 0.6\delta(x)$  and the sampling ratio is  $\alpha = 0.55$ . For the homogeneous matrix, the SE function  $\tau^{t+1} = S(\tau^t)/\alpha$  has two non-zero fixed points at  $\tau_{3,1}^* = 0.1619$ ,  $\tau_{3,2}^* = 0.01020$ . With the two-block matrix  $\gamma_1 = 0.847$ ,  $J_2 = 10^{-3}$ , the SE evolution  $\tau^{t+1} = M(\tau^t)/\alpha$  successfully removes the spurious fixed points and leads to perfect reconstruction.

proper choice of the rescaling parameter, the spurious fixed points of the SE equation will be removed so that perfect reconstruction is achievable. This is shown in Fig. 3 for the sparse signal. For signals which have no FOPT with the homogeneous Gaussian matrix, the dynamics of the two-block matrix keeps this property.

**Theorem 1.** *If the SE equation for signals with the homogeneous Gaussian matrix  $S(\tau)$  satisfies the no FOPT condition, then the SE equation for using the two-block matrix  $M(\tau)$  also satisfies the no FOPT condition.*

*Proof.* To prove the signal does not have FOPT with the two-block matrix, we only need to check the gradient of  $M(\tau)$ .

$$\kappa(\tau) = \frac{dM(\tau)}{d\tau} \quad (18)$$

$$= \gamma_1 \eta(\tau) + (1 - \gamma_1) \eta\left(\frac{\tau}{J_2}\right) \quad (19)$$

$$< \gamma_1 \frac{S(\tau)}{\tau} + (1 - \gamma_1) \frac{J_2}{\tau} S\left(\frac{\tau}{J_2}\right) \quad (20)$$

$$= \frac{M(\tau)}{\tau} \quad (21)$$

where the inequality is based on the no FOPT condition for the homogeneous matrix.  $\square$

### 3.3. The two-block matrix vs. the seeding matrix

The two-block matrix design is closely related to the seeding matrix with four sub-matrices. According to [4], the seeding matrix takes the form:

$$\Phi_s = \begin{pmatrix} \mathbf{G}_1 & \sqrt{J_2} \mathbf{G}_2 \\ \sqrt{J_1} \mathbf{G}_3 & \mathbf{G}_4 \end{pmatrix} \quad (22)$$

where  $\mathbf{G}_i$  is the homogeneous Gaussian matrix. For the seeding matrix to work it requires  $J_1 \gg J_2$ . If we set  $J_1 = 1/J_2$ , the

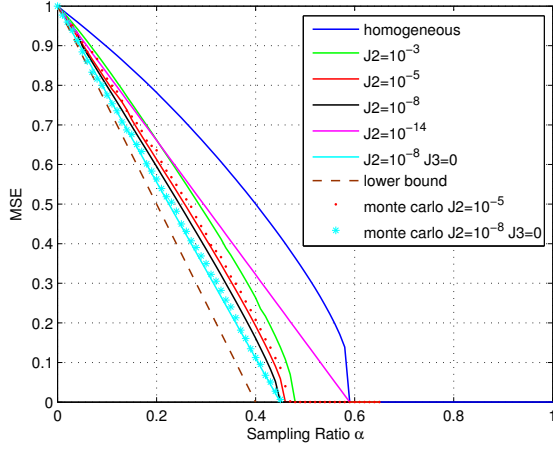


**Fig. 4.** The normalized SD function for the sparse signal with different measurement matrix configuration. For two-block matrix,  $\gamma_1 = \alpha/\alpha_c$  for  $\alpha < \alpha_c$ , where  $\alpha_{c1} = 0.59$  is the perfect reconstruction ratio for the homogeneous Gaussian matrix. The three-block matrix is achieved by convexifying the SD function of the two-block matrix with  $\gamma_1 = \frac{\alpha}{\alpha_{c1}}$ ,  $\gamma_2 = \frac{\alpha}{\alpha_{c2}} - \frac{\alpha}{\alpha_{c1}}$ ,  $\gamma_3 = 1 - \gamma_2 - \gamma_3$ , where  $\alpha_{c2} = 0.45$  is the perfect reconstruction ratio achieved by the two-block matrix.

two-block matrix  $\hat{\Phi}_M$  turns out to be the rescaled seeded matrix.

$$\hat{\Phi}_M = \begin{pmatrix} \mathbf{G}_1 & \sqrt{J_2}\mathbf{G}_2 \\ \mathbf{G}_3 & \sqrt{J_2}\mathbf{G}_4 \end{pmatrix} \quad (23)$$

$$= \begin{pmatrix} \mathbf{I}_1 & 0 \\ 0 & \sqrt{J_2}\mathbf{I}_4 \end{pmatrix} \Phi_s \quad (24)$$

where the index matrix  $\mathbf{I}_i$  has the same number of rows as  $\mathbf{G}_i$ .

The heuristics for the two-block matrix is that it simply shrinks a fraction of the signal to be very small. This leaves fewer large coefficients which can consequently be recovered through AMP. In the dynamics when the certainty for large coefficients is small enough, this acts as noise for the rescaled signal and the two part de-noise together. Compared to the seeding matrix, the two-block matrix has a relatively simple 1-D SE dynamics, which makes analytical optimization possible. The potential downside maybe the reduced robustness to noise.

#### 4. NUMERICAL SIMULATION

In this section we report the theoretical and empirical SD function with the two-block matrix for both sparse and compressible signals. To derive the empirical SD curves, the sparse signals were generated according to the Bernoulli-Gaussian model  $p(x)_{\text{BG}} = 0.4\mathcal{N}(x; 0, 1) + 0.6\delta(x)$ . The compressible signals were drawn from the two-state Gaussian mixture model  $p(x)_{\text{GM}} = 0.4\mathcal{N}(x; 0, 1) + 0.6\mathcal{N}(x; 0, 0.003)$ , which were motivated from the statistics of natural images. In all the empirical cases we used signals of length  $N = 5000$ . The distortion performance for each sampling ratio was averaged over 5000 problem realizations. Throughout, we assumed a noiseless scenario and used the GAMP algorithm with true signal distribution for reconstruction.

In Fig. 4, we plotted the average MSE against the sampling ratio for the sparse signal, under various choices of the rescaling parameter  $J_2$ . As the benchmark, we also showed the SD performance of

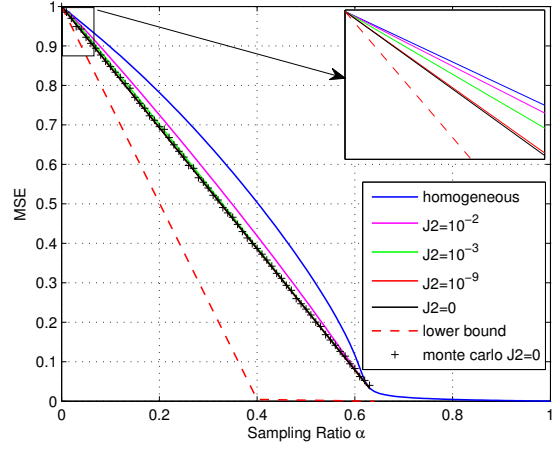


**Fig. 5.** The normalized SD function for the compressible signal with different measurement matrix configuration. For the two-block matrix,  $\gamma_1 = \alpha/\alpha_c$  for  $\alpha < \alpha_c$ , where  $\alpha_c = 0.63$  is the critical sampling ratio for the homogeneous Gaussian matrix.

the homogeneous Gaussian matrix and the model based bound [3]. With the two-block matrix we can accelerate the FOPT by decreasing  $J_2$ : the perfect reconstruction ratio is moved from 0.59 to 0.45 using  $J_2 = 10^{-8}$ . However, further shrinking of  $J_2$  does not improve the reconstruction to the optimal limit. We see some non-zero  $J_2$  delivers better SD performance than the hybrid zeroing matrix, with  $J_2 = 0$ .

One thing worth noting is that even with the improved performance, the two-block matrix still has a concave SD curve up to a new critical sampling ratio. A further convexified procedure with a three-block structure can then be easily applied to achieve even better reconstruction. In fact, if we introduce multiple  $J_i$ , we conjecture that this approach will tend to the optimal recovery as with the seeding matrix. Note again that for the multi-block matrix structure, the SE equation is still 1-D. The Monte Carlo simulation implies that for the finite size problem the SE prediction is accurate.

The SD functions, as well as the achievable model based bound for the compressible signal are shown in Fig. 5. Similarly to the sparse signal case, the two-block matrices outperform the homogeneous Gaussian matrix up to the critical sampling ratio  $\alpha_c$ . Also, the SD performance is better as we decrease  $J_2$ . We obtained an excellent agreement between the SD prediction and the Monte Carlo simulation. Empirically, we observed that the optimum weighting for  $J_2$  is zero for the compressible signal without FOPT. This suggests that without a FOPT the only gains come from the convexification of the SD function. However, the proof remains an open question.

#### 5. CONCLUSION

The main contribution of this paper is the introduction of the modulated matrix design. With the simple 1-D dynamics and the flexible rescaling matrix, it provides us a whole range of measurement matrix designs. As a special case, we understand the advantage and limitation of the two-block matrix based on the analysis of the first order phase transition. Further work involves parameter optimization and examination of multi-block modulated matrices. Different rescaling distribution in the stochastic setting also need to be considered.

## 6. REFERENCES

- [1] M.E. Davies and Chunli Guo, "Sample-distortion functions for compressed sensing," in *49th Annu. Allerton Conf. on Communication, Control, and Computing*. Monticello, IL, 2011, pp. 902–908.
- [2] Chunli Guo and M.E. Davies, "Sample allocation for statistical multiresolution compressed sensing," in *Acoustics, Speech and Signal Processing (ICASSP), 2012 IEEE International Conference on*, 2013.
- [3] Chunli Guo and M.E. Davies, "Sample distortion for compressed imaging," *accepted for publication in IEEE transactions of signal processing*, 2013.
- [4] F. Krzakala, M. Mézard, F. Sausset, Y. Sun, and L. Zdeborová, "Statistical-physics-based reconstruction in compressed sensing," *Phys. Rev. X*, vol. 2, pp. 021005(1–18), May 2012.
- [5] F. Krzakala, M. Mézard, F. Sausset, Y. Sun, and L. Zdeborová, "Probabilistic reconstruction in compressed sensing: Algorithms, phase diagrams, and threshold achieving matrices," *J. Stat. Mech.*, vol. P08009, Aug. 2012.
- [6] Jean Barbier, Florent Krzakala, Marc Mézard, and Lenka Zdeborová, "Compressed sensing of approximately-sparse signals: Phase transitions and optimal reconstruction," in *Communication, Control, and Computing (Allerton), 2012 50th Annual Allerton Conference on*. IEEE, 2012, pp. 800–807.
- [7] D. Donoho, A. Maleki, and A. Montanari, "Message passing algorithms for compressed sensing: I. motivation and construction," in *IEEE Inf. Theory Workshop (ITW)*. Dublin, Ireland, 2010, pp. 1–5.
- [8] Sundeep Rangan, "Generalized approximate message passing for estimation with random linear mixing," in *Information Theory Proceedings (ISIT), 2011 IEEE International Symposium on*. IEEE, 2011, pp. 2168–2172.